Nanoscale

PAPER

View Article Online
View Journal | View Issue

Cite this: *Nanoscale*, 2014, **6**, 7436

DNA and aptamer stabilized gold nanoparticles for targeted delivery of anticancer therapeutics†

Alfonso Latorre,‡[a] Christian Posch,‡[bc] Yolanda Garcimartín,[a] Anna Celli,[b] Martina Sanlorenzo,[bd] Igor Vujic,[bc] Jeffrey Ma,[b] Mitchell Zekhtser,[b] Klemens Rappersberger,[c] Susana Ortiz-Urda*[b] and Álvaro Somoza*[a]

Received 2nd January 2014
Accepted 19th April 2014

DOI: 10.1039/c4nr00019f

www.rsc.org/nanoscale

Gold nanoparticles (GNPs) can be used as carriers of a variety of therapeutics. Ideally, drugs are released in the target cells in response to cell specific intracellular triggers. In this study, GNPs are loaded with doxorubicin or AZD8055, using a self-immolative linker which facilitates the release of anticancer therapeutics in malignant cells without modifications of the active compound. An additional modification with the aptamer AS1411 further increases the selectivity of GNPs towards cancer cells. Both modifications increase targeted delivery of therapeutics with GNPs. Whereas GNPs without anticancer drugs do not affect cell viability in all cells tested, AS1411 modified GNPs loaded with doxorubicin or AZD8055 show significant and increased reduction of cell viability in breast cancer and uveal melanoma cell lines. These results highlight that modified GNPs can be functionalized to increase the efficacy of cancer therapeutics and may further reduce toxicity by increasing targeted delivery towards malignant cells.

Introduction

During the last few years, gold nanoparticles (GNPs) have attracted significant interest in the research community due to their remarkable physical and chemical properties. The optical and electronic characteristics, low cytotoxicity and high cell uptake capability provide an excellent platform for both therapeutic and diagnostic purposes.[1] Additionally, GNPs can be synthesized in different shapes and sizes and can easily be modified with biomolecules.[2–6] GNPs conjugated with oligonucleotides have particularly interesting properties due to the dense negative shell generated around the gold core: (i) the binding affinity by complementary oligonucleotides is enhanced by interstrand cooperative effects, (ii) incorporated DNA is stabilized and largely protected from nuclease degradation, and (iii) biocompatibility is improved compared to non-modified GNPs.[7–9] Moreover, in spite of their negative charge, GNPs show remarkable cellular uptake.[10]

The beneficial characteristics of GNPs have prompted the use of different oligonucleotide derivatives to achieve gene detection,[11] gene regulation[12] and targeted delivery.[13] Aptamers are single-stranded DNA or RNA molecules with specific secondary and tertiary conformations which facilitate the binding of matching target molecules with high selectivity and affinity. Starting in the early 1990s, the directed discovery of specific aptamers, such as AS1411, has rendered remarkable improvements of targeted delivery of nanoparticles. AS1411 is a G-rich aptamer with strong affinity to the protein nucleolin, which is mainly found in the nucleus of cells, but is translocated and shows increased surface expression in malignant cells.[14,15] The high binding affinity of AS1411 to nucleolin promotes cell uptake of AS1411 modified nanostructures and has previously been used to enable the detection and treatment of malignant cells with magnetic or PLGA–PEG nanoparticles.[16,17]

An additional beneficial feature of oligonucleotide modified GNPs is their high solubility in water, buffers and cell culture media without loss of stability. This property in conjunction with the drug-loading capacities of nanoparticles has allowed the delivery and distribution of hydrophobic chemotherapeutic drugs such as paclitaxel, whose effectiveness is limited by its low solubility in aqueous solutions.[18,19]

Recent developments in targeted therapy for various malignancies have not only increased response rates, but also show favorable side effect profiles compared to traditional anticancer therapeutics. The use of self-immolative linkers for the controlled release of a substrate is one of the strategies to further increase the specificity and reduce toxicity.[20] Different stimuli such as temperature, pH and reductive environment can trigger the release selectively inside the cell.[21]

[a]*Instituto Madrileño de Estudios Avanzados en Nanociencia, CNB-CSIC-IMDEA Nanociencia Associated Unit, Cantoblanco, Madrid, Spain. E-mail: alvaro.somoza@imdea.org*

[b]*University of California San Francisco, Mount Zion Cancer Research Center, San Francisco, USA*

[c]*The Rudolfstiftung Hospital, Vienna, Austria*

[d]*Department of Medical Sciences, Section of Dermatology, University of Turin, Italy*

† Electronic supplementary information (ESI) available. See DOI: 10.1039/c4nr00019f

‡ Contributed equally to this work.

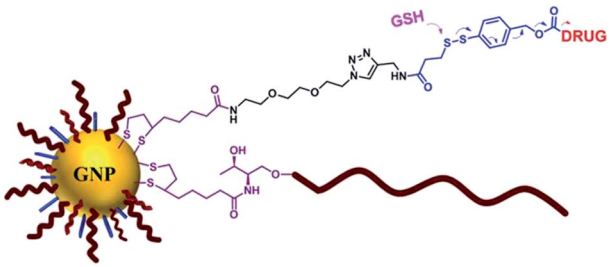

Fig. 1 Schematic representation of DNA stabilized GNPs loaded with drug. DNA (red line) is conjugated through a dithiolane linker (purple). The drug is conjugated through a bifunctional linker composed of an anchoring dithiolane moiety (purple) and self-immolative spacer (blue). The release of doxorubicin (DOX) or AZD8055 is triggered by glutathione (GSH) breaking the disulfide group and promoting an electronic movement by the π cloud rendering the release of CO_2 and the therapeutic in a 1,6-benzyl elimination reaction.

Encouraged by the unique characteristics of DNA conjugated GNPs as a drug delivery system and the specific interaction of aptamers like AS1411 with cancer cells, we describe DNA stabilized GNPs for targeted delivery of chemotherapeutic doxorubicin (DOX) and the small molecule inhibitor of PI3K and mTOR isoforms AZD8055 (AZD). GNPs were evaluated in primary human keratinocytes, MCF-7 breast cancer cells as well as uveal melanoma cell lines OMM1.3 and Mel202. DOX and AZD were attached to GNPs using a bifunctional linker containing a dithiolane and a self-immolative disulfide based structure. Dithiolane allows attachment of drugs onto the gold surface and the self-immolative fragment facilitates the release of drugs upon an intracellular stimulus. The release is triggered by the presence of reductive agents such as glutathione (GSH), which is present in a 1000-fold higher concentration intracellularly, compared to the extracellular environment and present in higher concentrations in malignant cells compared to normal cells. Disulfide cleavage promotes an electronic movement by the π cloud rendering the release of CO_2 and DOX or AZD in a 1,6-benzyl elimination reaction,[22] disassembling the anticancer therapeutic from the GNP without chemical modifications of the active compound (Fig. 1).

In order to preserve the stability of GNPs loaded with doxorubicin or AZD8055, various oligonucleotide sequences were used in order to test their influence on GNP stability, drug release, cell uptake and toxicity. Additionally, the aptamer AS1411 was used to achieve targeted drug delivery with GNPs, showing increased activity only in malignant cells MCF-7, OMM1.3 and Mel202, but not in primary human keratinocytes.

Results

Modified GNPs are stable and incorporate high amounts of doxorubicin

DNA stabilized GNPs were synthesized using oligonucleotides bearing a dithiolane modification at the 3′end. The dithiolane moiety allowed the functionalization of GNPs due to the high affinity of sulfur to gold. GNPs stabilized with different DNA strands were loaded with DOX using immolative linkers and evaluated for drug loading and stability. Nanostructures bearing Poly-T (15nt) nucleotides were able to incorporate up to 2900 times the equivalent of free DOX molecules (9 nM Poly-T–DOX GNPs holding 26.1 μM DOX). The characteristic plasmon resonance band at 520 nm when dispersed in an aqueous solution confirmed that GNPs did not aggregate. Poly-T–DOX GNPs showed a plasmon band similar to non-modified GNPs, adding evidence that the modifications of the GNPs do not impair characteristics and stability in aqueous solution. Additionally, this nanostructure also showed great stability after dispersion in PBS buffer (Fig. S1†). We also tested the effect of GNPs functionalized with different oligonucleotides such as Poly-A, Poly-C, and a scramble sequence of fifteen nucleotides (SCR-15). DOX concentrations loaded onto the different GNP designs ranged from 2255 fold to 3922 fold the equivalent of free DOX (9 nM GNPs holding 20.3 to 35.3 μM of DOX). Transmission electron microscopy (TEM) images of selected GNPs are provided in the ESI (Fig. S2†).

Stability of structures varied across the different GNP designs and was primarily related to the employed oligonucleotide sequences (Table S1†). The UV/VIS spectra showed a slight red shift of the plasmon band for Poly-C nanostructures, indicating their aggregation. Poly-A oligonucleotides showed the lowest capacity to stabilize GNPs, with a less intense and more red shifted plasmon band compared to all other designs (Fig. 2).

Dynamic light scattering confirmed UV/VIS results with Poly-T–DOX GNPs having the smallest hydrodynamic size and Poly-A–DOX GNPs having the largest. Interestingly, when comparing the dispersion of GNPs in water or PBS buffer, the hydrodynamic size of the nanoparticles was largely unaffected (Fig. S3†).

The low stability of GNPs modified with polyadenine sequences (Poly-A) could be due to the high affinity of polyadenine sequences to gold nanoparticles. This feature has been used previously to modify gold nanoparticles with oligonucleotides and might, in our case, increase the interaction between particles leading to aggregation.[23]

Oligonucleotide length and aptamer modification do not influence the GNP stability

To explore the influence of the oligonucleotide length on GNP stability, SCR sequences of 15 (SCR-15) and 30 (SCR-30)

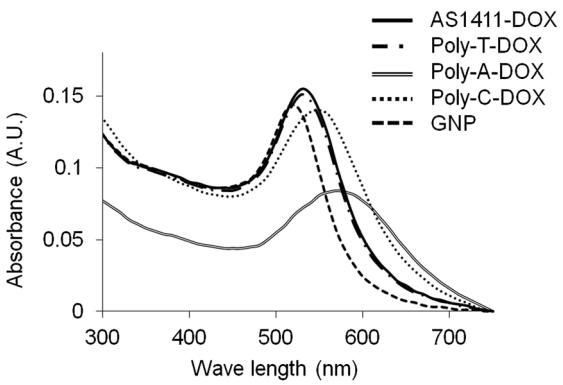

Fig. 2 UV/VIS spectra of Poly-T–DOX, Poly-A–DOX, Poly-C–DOX, AS1411–DOX and GNPs without DOX resuspended in water. The red shift of Poly-A–DOX nanoparticles indicates their aggregation.

nucleotides were used. We did not observe differences in stability among nanostructures modified with oligonucleotides of either 15 or 30 bases, suggesting a negligible influence of the oligonucleotide length on GNP stability (Fig. S3 and S4†). In the next set of experiments, the aptamer AS1411 was used to stabilize GNPs. To favor the binding properties of the aptamer, a 6T spacer was introduced at the 3′end between the thiolane modification and the AS1411 sequence to yield an oligonucleotide of 32 bases composed exclusively of T and G nucleotides. The 6T spacer was chosen based on the findings that Poly-T modifications were the most stable. Using AS1411, we could load up to 20.8 μM of DOX onto 9 nM GNPs with high stability. The UV/VIS spectra and hydrodynamic size showed similar values and were comparable to the results found with Poly-T–DOX nanostructures (Fig. 2 and S3†).

The intracellular environment triggers the cleavage of the self-immolative linker

All modified GNPs were tested for their ability to release DOX upon the disassembly of the self-immolative disulfide based linker, triggered by GSH. To assess DOX release from GNPs, fluorescent emission of DOX was monitored. In the absence or at low concentrations of GSH, the fluorescent signal of DOX is quenched through an energy transfer process between DOX and the GNP. As DOX is released from the GNP due to the presence of GSH, an increase of fluorescence can be observed. A 1 nM solution of Poly-T–DOX GNPs in PBS was incubated with either 1 μM GSH resembling the extracellular environment, or 1 mM GSH resembling the intracellular environment. Changes of fluorescence intensity were measured over time. We noticed a marked increase of fluorescence with 1 mM GSH, whereas fluorescence of GNPs incubated with 1 μM GSH was negligible (Fig. 3).

Next, we compared the DOX release of different designs of GNPs (Poly-T, Poly-A, Poly-C, SCR-15, SCR-30 and AS1411). A 1 nM solution of DOX-GNPs was incubated with 1 mM GSH and the increase of the fluorescence was monitored over time. Results showed that most of the DOX is released within the first 20 h for all nanostructures (Fig. S5†).

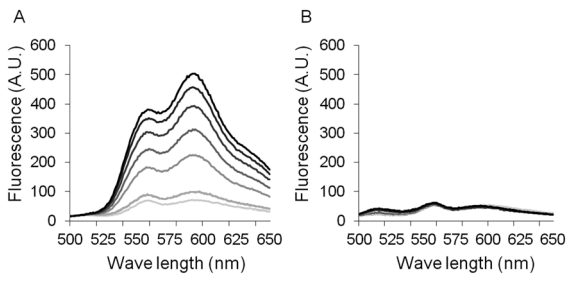

Fig. 3 Glutathione (GSH) triggers the release of doxorubicin (DOX) from GNPs. (A) Poly-T–DOX GNPs (1 nM) gave a strong fluorescent signal when incubated with 1 mM GSH. (B) Fluorescence of GNPs incubated with 1 μM GSH remained at the base line and was unchanged over time. Peak fluorescence was recorded after 180 minutes (top, black lines). Lines in different gray scales represent shorter incubation periods.

Aptamer modifications selectively increase incorporation of GNPs in cancer cells

To compare the uptake of modified GNPs in living cells, nanostructures were incubated with the human breast cancer cell line MCF-7, the human melanoma cell lines OMM1.3 and Mel202 and early passage, primary human keratinocytes. Analyzes by flow cytometry revealed that all nanostructure designs gave a fluorescent signal indicating the release of DOX. The length of the oligonucleotide sequence did not influence the DOX release (Fig. S6†). As shown in Fig. 4, the strongest fluorescent signal was obtained when AS1411-GNPs were used with the malignant cell lines MCF-7, OMM1.3 and Mel202. In contrast, AS1411–DOX GNPs did not increase fluorescence in primary human keratinocytes confirming the influence of the aptamer to selectively increase uptake in cancer cells (Fig. 4).

Confocal imaging of cells revealed that GNPs reached the cytoplasm of cells. Images are suggestive of clustering of nanostructures, which may be due to the previously described endocytic uptake of GNPs by cells and intracellular accumulation of nanoparticles (Fig. 5 and S7†).[24]

Doxorubicin and AZD8055 loaded, aptamer modified GNPs selectively reduce cell viability

DOX loaded GNPs reduced the viability in a dose dependent manner. AS1411–DOX-GNPs were more potent reducing cell viability in cancer cell lines MCF-7, OMM1.3 and Mel202 than DOX-GNPs without AS1411 modification (Fig. 6). Noticeably, GNPs bearing aptamers did not further reduce the viability in primary human keratinocytes.

As targeted inhibitors are becoming an essential focus of anticancer therapy, we would like to prove if our modified GNPs might also be used for the selective delivery of small molecule inhibitors. We loaded AZD8055 (AZD), a selective inhibitor of mTOR kinases, onto AS1411 modified GNPs.[25] Similar to the nanostructures loaded with DOX, AZD bearing GNPs were stable in PBS (Fig. S8†). The hydrodynamic size and TEM

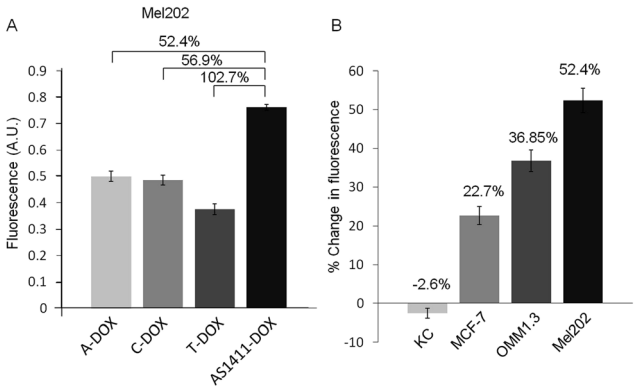

Fig. 4 Fluorescence of different GNP designs measured by flow cytometric analysis. Increased fluorescence with AS1411 modified GNPs compared to all other designs (cell line Mel202) (A). The aptamer AS1411 increases the GNP uptake in all malignant cells (MCF-7, OMM1.3 and Mel202) but not in primary human keratinocytes (KC) (B). ($N = 3$, error bars indicate the standard deviation.)

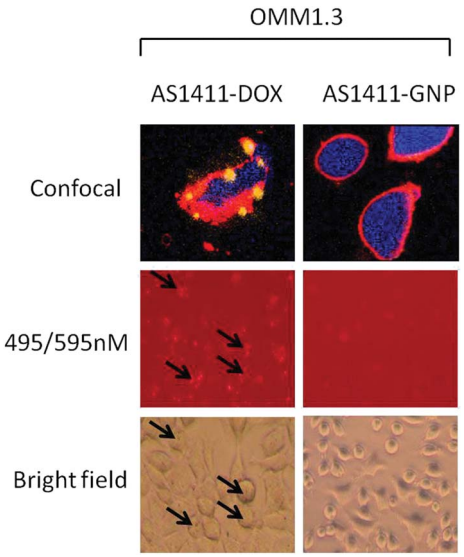

Fig. 5 Microscopic pictures of the uveal melanoma cell line OMM1.3 incubated with GNPs. Confocal images confirm that the AS1411–DOX-GNPs reach the cytoplasm and release DOX (yellow) (deep red membrane stain, DAPI counter stain). DOX releasing GNPs can also be seen inside the cells with a fluorescence microscope (arrows, excitation 495 nm, emission 595 nm). The corresponding bright field picture of OMM1.3 cells.

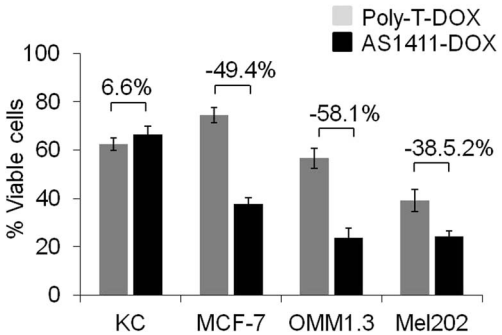

Fig. 6 GNPs loaded with DOX decrease the cell viability. The use of the aptamer AS1411 for GNP modification increased the selectivity for malignant cells and further decreases the cell viability compared to Poly-T modified GNPs in all malignant cell lines (MCF-7, OMM1.3 and Mel202) but not in primary human keratinocytes (KC). ($N = 3$, error bars indicate the standard deviation.)

characterization can be found in the ESI (Fig. S2 and S9†). All particles were active with those bearing the AS1411 aptamer modification showing selective targeting of malignant cells. Cell viability decreased to a greater extent with AS1411–AZD-GNPs in all 3 cancer cell lines tested when compared to non-malignant cells (keratinocytes) or GNPs not bearing the AS1411 modification (Fig. 7).

Discussion

In this work we present a new approach for the synthesis of modified GNPs bearing oligonucleotides and anticancer

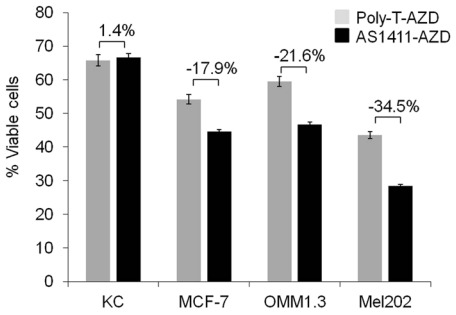

Fig. 7 AS1411–AZD-GNPs reduce the cell viability. GNPs were loaded with AZD8055, a selective inhibitor of PI3K and mTOR isoforms. The modification with the aptamer AS1411 further decreased the cell viability in all malignant cell lines (MCF-7, OMM1.3 and Mel202) but not in primary human keratinocytes (KC). ($N = 3$, error bars indicate the standard deviation.)

therapeutics. The conjugation with GNPs is achieved using a dithiolane moiety, which has two advantages compared to other thiol groups commonly used in the preparation of modified oligonucleotides: (i) removal of thiol-protecting groups from oligonucleotides is not required and (ii) binding is fast and stability of modified GNPs is increased.[26] Using the anchoring dithiolane moiety in combination with a self-immolative spacer we are further able to attach and selectively release anticancer therapeutics such as DOX or the small molecule inhibitor AZD8055 from oligonucleotide modified GNPs. Previous studies have demonstrated that GNPs can be loaded with anticancer therapeutics, however, the conjugation process implies that drugs are released with chemical modifications. In contrast, our release system is triggered by reducing agents such as GSH and the released drug is not modified and present in its FDA or EMA approved and most active form. The increase of fluorescence when DOX modified GNPs are incubated with 1 mM GSH provides evidence that the linker is activated under conditions similar to the intracellular environment.[27,28] This is further supported by confocal imaging, showing the disassembly of GNPs upon cell internalization. Importantly, the strongest fluorescent signal is obtained when aptamer modified GNPs (AS1411-GNPs) are used with the malignant cell lines MCF-7, OMM1.3 and Mel202. In contrast, primary human keratinocytes do not show an increase of fluorescence. We interpret this result as being a consequence of a greater GNP uptake due to the high affinity of the aptamer AS1411 to nucleolin, which is expressed on the surface of malignant cells, allowing for targeted delivery of GNPs.[14,15] Additionally, drugs are preferentially released in malignant cells due to higher concentrations of GSH in cancer cells compared to normal cells.[28] GSH measurements in cells used for this study are provided in the ESI (Fig. S10†). Concomitant with higher levels of fluorescence, malignant cells showed a significant greater reduction of cell viability when AS1411 modified DOX-GNPs were used. This reduction in cell viability is caused by the released anticancer therapeutics. Different designs of modified GNPs not loaded with DOX have no effect on cell viability and can be considered non-toxic (Fig. S11†).[24]

In the last two decades, small molecule inhibitors have enriched the armory of clinicians to treat cancer patients, resulting in remarkable response rates and improved overall survival.[25,29,30] The concept of pathway inhibition with specific inhibitors for currently 'un-druggable' oncogenes like GNAQ or NRAS is becoming increasingly common.[29,31] However, pathway interference with inhibitors can only in part be considered a tumor specific therapy as many other cell types also use those signaling cascades for survival and growth. Although cancer cells over activate certain pathways, several other tissues, especially those with a high proliferative index, will be affected by treatment, potentially causing severe adverse effects. For this reason we loaded AZD8055, a selective inhibitor of mTOR kinases currently used in several clinical trials for cancer treatment, onto AS1411 modified GNPs to specifically deliver the anticancer agent to malignant cells.[25] Indeed, we are able to reduce viability in the malignant cells MCF-7, OMM1.3 and Mel202 to a greater extent compared to normal cells, similar to results obtained with DOX loaded GNPs. This study provides evidence that our GNP design allows for increasing specificity in the delivery of anticancer therapeutics combining the features of malignant cell recognition with aptamers, as well as preferential drug release in malignant cells due to the self-immolative release system. We believe that this concept has great potential to optimize cancer therapy and improve the side effect profile for therapeutics currently used for pathway inhibition in cancer.

Conclusions

In this work, we were able to show that GNPs can be facilitated to selectively deliver different anticancer drugs including small molecule inhibitors to malignant cells. Specificity is increased by aptamer mediated cell recognition and by the preferential release of anticancer therapeutics in malignant cells. The technology presented is robust, yields stably modified GNPs and can potentially be applied to optimize the side effect profile and efficacy of several anticancer therapeutics in the near future.

Methods

Materials

The UV/VIS spectra were recorded at room temperature with a Synergy H4 microplate reader. Fluorescence spectra were recorded at room temperature with a FluoroMax-4 fluorimeter using 1 cm path length quartz cells. Ultrapure reagent grade water (18.2 MΩ, Wasserlab) was used in all experiments.

Synthesis of oligonucleotides

Oligonucleotides were prepared with a MerMade4 DNA Synthesizer using phosphoramidites (Link Technologies) and a modified CPG (see ESI†). After solid-phase synthesis, the solid support was transferred to a screw-cap glass vial and incubated at room temperature for 16 h with 2 mL of ammonia solution (33%). After the vial was cooled on ice, the supernatant was transferred into micro-centrifuge tubes and both the solid support and vial were rinsed with water. The combined solutions were dried in an evaporating centrifuge. The samples were purified by 20% polyacrylamide gel electrophoresis and oligonucleotides were eluted from gel fractions using an elutrap system. The solutions were desalted using NAP-10 columns and concentrated in an evaporating centrifuge.

Preparation of DNA stabilized GNPs loaded with doxorubicin

Gold nanoparticles were synthesized following the Turkevich protocol.[22,32,33] In brief, a 100 mL water solution of $HAuCl_4$ (34 mg) was refluxed at 140 °C and reduced for 15 min with a solution of sodium citrate (118 mg) in water (10 mL). The concentration of GNPs was determined by UV/VIS spectrometry using Beer's law: $\lambda = 520$ nm, $\varepsilon = 2.7 \times 108\ M^{-1}\ cm^{-1}$. To synthesize DNA stabilized GNPs loaded with DOX, 1 mL of GNPs were incubated with modified oligonucleotides (17 nmol). After 20 min, NaCl 5 M (20 μL) was added and stirred for 10 min. Then, 40 μL of a solution of modified DOX in DMF (2.3 mM) was added and stirred for 16 h. Details on the preparation are provided in the ESI.† Finally, GNPs were centrifuged at 13 200 rpm at 4 °C, the supernatant was removed and the reddish pellet was resuspended in water. This process was repeated three times to remove unattached DNA and modified DOX.

Release and quantification of doxorubicin conjugated on GNPs

The release of DOX was evaluated using fluorescence spectrometry. 150 μL of DNA stabilized GNPs loaded with DOX were diluted with 1345 μL of PBS and 15 μL of GSH 100 mM. Then, the increase of fluorescence was monitored at different time intervals ($\lambda_{exc} = 495$ nm, $\lambda_{em} = 595$ nm). The concentration of DOX was determined with a similar protocol. 150 μL of DNA stabilized GNPs loaded with DOX were diluted with 1342.5 μL of PBS and 7.5 μL of DTT 1M. The mix was stirred for 16 h followed by measurement of fluorescence at $\lambda_{exc} = 495$ nm, $\lambda_{em} = 595$ nm. The concentration was calculated by interpolation from a standard linear calibration curve.

In order to quantify the loading of oligonucleotides onto the nanoparticles, DNA strands were labeled with a fluorescein molecule at the 5′ end. After conjugation with the nanostructures, fluorescence of the supernatant was quantified ($\lambda_{exc} = 470$ nm, $\lambda_{em} = 520$ nm) to determine the loading efficacy.

Hydrodynamic size

The hydrodynamic size was determined by dynamic light scattering (DLS) using a Zetasizer Nano (Malvern). 5 μL of GNPs were diluted in 200 μL PBS. The size measurements were performed at 25 °C at a 173° scattering angle in disposable microcuvettes. The mean dynamic diameter was determined by cumulative analysis.

TEM pictures

Transmission electron microscopy images were generated using a JEOL JEM 101 microscope operating at 100 keV. Samples were prepared by placing one drop of a dilute suspension in water

onto a carbon coated copper grid and leaving it to dry at room temperature.

Cell lines and cell culture

The human breast cancer cell line MCF-7 and human melanoma cell lines OMM1.3 and Mel202 were a generous gift from James E. Cleaver and Boris Bastian at the University of California, San Francisco. Both cell lines were maintained in RPMI 1640 media supplemented with 10% FBS. Early passage, primary human keratinocytes were available in our laboratory and maintained in a medium containing equal parts of supplemented Medium 154 (Life Technologies, M-154-500) and supplemented Keratinocyte-SFM (Life Technologies, 17005-042). All cell lines were incubated at 37 °C under 5% CO_2.

Cell viability assays

All viability assays were at least carried out in triplicates. The relative number of viable cells was calculated using CellTiter-Glo® (Promega, G7570) after 72 h of incubation under the indicated conditions. The total luminescence was measured on the SynergyHT plate reader (BioTek) using Gen5 software (Version 1.11.5). Cells were treated with the indicated GNPs in concentrations ranging from 1.5 μM to 375 nM.

Flow cytometry

Cells were plated in 24 well plates at sub-confluent levels. After 24 h, the medium was replaced by complete media containing 1 nM GNPs and incubated at 37 °C for 2 h. Then, cells were washed to remove unbound nanoparticles and incubated with the complete medium for 24 h at 37 °C. Cells were detached with 0.05% trypsin and analyzed with the AccuriC6 Flow Cytometer® using the CFlow® software (Version 1.0.227.4).

Confocal imaging

Cells were grown in 2-well glass chamber slides at sub-confluent levels and incubated with 3 nM GNPs. Cells were treated in the same manner as described for flow cytometry. Before imaging, cells were stained with CellMask Deep Red Plasma membrane Stain (Life Technologies, C10046) and DAPI (Vector, H-1200). Images were taken with the Zeiss Confocal Laser-Scanning Microscope (LSM 510) using a 63× oil immersion objective with a 1.4 NA. The filter sets and laser lines used were: CellMask Deep Red Plasma membrane Stain: excitation 633 nm, BP 650–710; doxorubicin: excitation 543 nm, BP 565–615; DAPI: ti:Saph excitation 800 nm, BP390–465.

Acknowledgements

The authors thank J. E. Cleaver and B. Bastian for providing the cell lines used in this study. The authors further thank G. Monico, G. Ow, K. Lai, D. V. Arneson, V. Feichtenschlager, D. Gho, S. Kim, A. Yen and K. Johnston for helpful advice and discussion in the elaboration of this manuscript. The authors thank T. Dattels for his generous support and Gorka Salas for taking TEM pictures. This work has been supported by the Melanoma Research Alliance, the Dermatology Foundation, the American Skin Association, the American Cancer Association, the Max Kade Foundation, the Verein für Dermatologie Krankenanstalt Rudolfstiftung and the René Touraine Foundation. The Spanish Ministry of Science and Innovation (Grant: SAF2010-15440) and IMDEA Nanociencia are also acknowledged for financial support.

Notes and references

1 A. J. Mieszawska, W. J. M. Mulder, Z. A. Fayad and D. P. Cormode, *Mol. Pharmaceutics*, 2013, **10**, 831–847.
2 M. R. Langille, M. L. Personick, J. Zhang and C. A. Mirkin, *J. Am. Chem. Soc.*, 2012, **134**, 14542–14554.
3 G. Zhou, Y. Liu, M. Luo, X. Li, Q. Xu, X. Ji and Z. He, *Langmuir*, 2013, **29**, 4697–4702.
4 S. Dominguez-Medina, J. Blankenburg, J. Olson, C. F. Landes and S. Link, *ACS Sustainable Chem. Eng*, 2013, **1**, 833–842.
5 O. V. Gnedenko, Y. V. Mezentsev, A. A. Molnar, A. V. Lisitsa, A. S. Ivanov and A. I. Archakov, *Anal. Chim. Acta*, 2013, **759**, 105–109.
6 S. Bhattacharya and A. Srivastava, *Langmuir*, 2003, **19**, 4439–4447.
7 A. K. R. Lytton-Jean and C. A. Mirkin, *J. Am. Chem. Soc.*, 2005, **127**, 12754–12755.
8 J. W. Zwanikken, P. Guo, C. A. Mirkin and M. Olvera de la Cruz, *J. Phys. Chem. C*, 2011, **115**, 16368–16373.
9 M. D. Massich, D. A. Giljohann, A. L. Schmucker, P. C. Patel and C. A. Mirkin, *ACS Nano*, 2010, **4**, 5641–5646.
10 D. A. Giljohann, D. S. Seferos, P. C. Patel, J. E. Millstone, N. L. Rosi and C. A. Mirkin, *Nano Lett.*, 2007, **7**, 3818–3821.
11 Y. Tu, P. Wu, H. Zhang and C. Cai, *Chem. Commun.*, 2012, **48**, 10718–10720.
12 A. E. Prigodich, D. S. Seferos, M. D. Massich, D. A. Giljohann, B. C. Lane and C. A. Mirkin, *ACS Nano*, 2009, **3**, 2147–2152.
13 Y.-L. Luo, Y.-S. Shiao and Y.-F. Huang, *ACS Nano*, 2011, **5**, 7796–7804.
14 P. J. Bates, D. A. Laber, D. M. Miller, S. D. Thomas and J. O. Trent, *Exp. Mol. Pathol.*, 2009, **86**, 151–164.
15 S. Soundararajan, L. Wang, V. Sridharan, W. Chen, N. Courtenay-Luck, D. Jones, E. K. Spicer and D. J. Fernandes, *Mol. Pharmacol.*, 2009, **76**, 984–991.
16 J. K. Kim, K.-J. Choi, M. Lee, M. Jo and S. Kim, *Biomaterials*, 2012, **33**, 207–217.
17 J. Guo, X. Gao, L. Su, H. Xia, G. Gu, Z. Pang, X. Jiang, L. Yao, J. Chen and H. Chen, *Biomaterials*, 2011, **32**, 8010–8020.
18 J. D. Gibson, B. P. Khanal and E. R. Zubarev, *J. Am. Chem. Soc.*, 2007, **129**, 11653–11661.
19 D. N. Heo, D. H. Yang, H.-J. Moon, J. B. Lee, M. S. Bae, S. C. Lee, W. J. Lee, I.-C. Sun and I. K. Kwon, *Biomaterials*, 2012, **33**, 856–866.
20 C. A. Blencowe, A. T. Russell, F. Greco, W. Hayes and D. W. Thornthwaite, *Polym. Chem.*, 2011, **2**, 773–790.
21 S. Ganta, H. Devalapally, A. Shahiwala and M. Amiji, *J. Controlled Release*, 2008, **126**, 187–204.
22 S. Zalipsky, N. Mullah, C. Engbers, M. U. Hutchins and R. Kiwan, *Bioconjugate Chem.*, 2007, **18**, 1869–1878.

23 H. Pei, F. Li, Y. Wan, M. Wei, H. Liu, Y. Su, N. Chen, Q. Huang and C. Fan, *J. Am. Chem. Soc.*, 2012, **134**, 11876–11879.
24 R. Shukla, V. Bansal, M. Chaudhary, A. Basu, R. R. Bhonde and M. Sastry, *Langmuir*, 2005, **21**, 10644–10654.
25 C. Bartholomeusz and A. M. Gonzalez-Angulo, *Expert Opin. Ther. Targets*, 2012, **16**, 121–130.
26 J. A. Dougan, C. Karlsson, W. E. Smith and D. Graham, *Nucleic Acids Res.*, 2007, **35**, 3668–3675.
27 N. Ballatori, S. M. Krance, S. Notenboom, S. Shi, K. Tieu and C. L. Hammond, *Biol. Chem.*, 2009, **390**, 191–214.
28 J. M. Estrela, A. Ortega and E. Obrador, *Crit. Rev. Clin. Lab. Sci.*, 2006, **43**, 143–181.
29 C. Posch, H. Moslehi, L. Feeney, G. A. Green, A. Ebaee, V. Feichtenschlager, K. Chong, L. Peng, M. T. Dimon, T. Phillips, A. I. Daud, T. H. McCalmont, P. E. Leboit and S. Ortiz-Urda, *Proc. Natl. Acad. Sci. U. S. A.*, 2013.
30 A. Stoffel, *BioDrugs*, 2010, **24**, 303–316.
31 C. Posch and S. Ortiz-Urda, *OncoTargets Ther.*, 2013, **4**, 494–495.
32 J. Kimling, M. Maier, B. Okenve, V. Kotaidis, H. Ballot and A. Plech, *J. Phys. Chem. B*, 2006, **110**, 15700–15707.
33 J. Turkevich, P. Stevenson and J. Hillier, *Discuss. Faraday Soc.*, 1951, **11**, 55–75.